Analysis of an controller design for an electro-hydraulic servo pressure regulator

Pedersen, Henrik C.; Andersen, Torben Ole; Madsen, A. M.; Dahl, M.; Nielsen, B.K.; Stubkier, Søren

Published in:
Proceedings of the 10th International Workshop on Research and Education in Mechatronics, REM2009

Publication date:
2009

Document Version
Publisher's PDF, also known as Version of record

10th International Workshop on Research and Education in Mechatronics
September 10^{th}-11^{st} 2009, Glasgow,UK

Analysis of and Controller Design For An Electro-Hydraulic Servo Pressure Regulator

Henrik C. Pedersen[1], Torben O. Andersen[1], Søren Stubkier[2],
Andreas N. Madsen[3], Mads Dahl[4], Brian K. Nielsen[2]

[1]*Aalborg University, Department of Energy Technology, DK-9210 Aalborg East, Denmark*
[2]*Sauer-Danfoss ApS, DK-6430 Nordborg, Denmark*
[3]*Hydac, DK-5550 Langeskov, Denmark*
[4]*Serman & Tipsmark A/S, DK-9700 Brønderslev, Denmark*

Abstract: Mobile hydraulics is in a transition phase, where electronic sensors and digital signal processors are starting to become standard on a high number of machines, hereby replacing hydraulic pilot lines and offering new possibilities with regard to both control and feasibility. For controlling some of the existing hydraulic components there are, however, still a need for being able to generate a hydraulic pilot pressure, as e.g. almost all open-circuit pumps are hydraulically controlled. The focus of the current paper is therefore on the analysis and controller design an electro-hydraulic servo pressure regulator, which generates a hydraulic LS-pressure based on an electrical reference, hereby synergistically integrating knowledge from all parts of the mechatronics area.

The servo pressure regulator is used to generate the LS-signal for a variable displacement pump, and the paper first presents the considered system and an experimentally verified model of this. A linearized model is then presented, which comprise the basis for a stability and sensitivity analysis of the system. Based on the results of the analysis, a control strategy is designed in combination with optimisation of the mechanical design to generate a controlled leakage flow that aids in stabilising the system. The robustness of the system is then discussed in relation to different pilot line volumes and pump dynamics. Finally experimental results are presented, where the performance is compared to that of a similar hydraulic reference system, which has been the basis for the specification of performance requirements.

Keywords: Hydraulics, Mechanics, Electronics, Controller Design, Modelling, Stability, Sensitivity

I Introduction

The development of hydraulic systems shows a clear tendency towards electrically controlled components, as pointed out by e.g. [3]. This also means that the need for hydraulic pilot lines are decreased. However in the transition phase between traditionally hydraulically controlled components and fully electrically controlled systems there may be a need for generating some of the pilot pressures based on electrical systems. One example on this problem is hydraulic LS-pumps connected to an otherwise electronically controlled system (valves, engine etc.), where there is no hydraulic LS-pressure available. This problem is the objective of the current paper, where focus is on controlling the LS-pressure for the pump based on the electric LS reference signal, for which a hydraulic copy is generated using a small spool valve, further on denoted a servo pressure regulator.

To the knowledge of the authors, no other such solution exist, although the control problem has some resemblence to controlling the pump pressure in an ELS-system, see e.g. [5, 2, 6, 9, 10, 1]. Common for these studies are that they have used a sufficiently fast servo valve/proportional valve for obtaining the electrical control of the pump, directly controlling the flow to the displacement piston of the pump, hereby removing the original hydro-mechanical LS-regulator in the pump and hence, in effect replacing the dynamics of the hydro-mechanical LS-regulator and pilot line by that of the inserted valve and controller. In the current paper the hydro-mechanical regulator in the pump is still included, and the objective is in-

stead to generate the LS-pressure using a spool valve, taking into account a given pump dynamic. A similar idea of using an artifically generated LS-pressure has been presented by [4] as part of a pump regulator, where the LS-pressure was generated based on the pump pressure using a series connection consisting of a fixed orifice and electrically controlled relief valve, hereby obtaining the effect of a pressure divider. Apart from the idea of generating the LS-pressure based on the pump pressure, the two solutions do however pose quite different problems not only due to different topologies and control problems, but also as the presented solution is intended to be mounted a distance away from the pump and should be applicable in combination with a large variation of pumps.

verified model of this. A linearised model is derived, which comprise the foundation for a stability analysis of the system presented, and a discussion of the sensititivy of the system to varying operating conditions. Based on the results of this analysis the controller design is presented and robustness evaluated. Finally both simulation and experimental results are presented, and the performance of the electro-hydraulic pressure regulator is compared to that of the hydraulic reference system.

II System Modelling

The system considered is shown in Fig. 1 and consists of the pump, spool valve, hoses and the load system. This setup may both be used as a classical LS-system (reference system) or with the pressure regulator, making it possible to test the two systems individually.

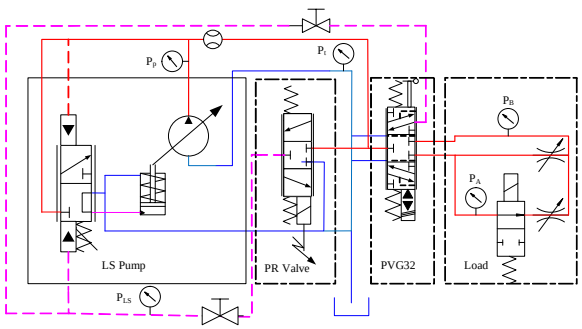

Figure 1: Diagram of the experimental set-up.

The system consists of a $57[cm^3]$ Sauer-Danfoss serie 45 H-frame pump, a load system consisting of a PVG 32 pressure compensated proportional valve, two variable orifices connected in parallel and an on-off valve. The servo pressure regulator is designed as a 3/3-NC null lap spool valve. It is actuated with a voice coil which is connect to a DC/DC inverter, by which it is also possible to current control the voice coil. The setup may manually be switched between the two systems using the two ball valves.

Considering first the spool valve a model view of this is shown in Fig. 2 with indication of the used notation. The purpose of the valve is to control the flow to or from the (dashed) pilot line (see Fig. 1), hereby generating the hydraulic LS-pressure.

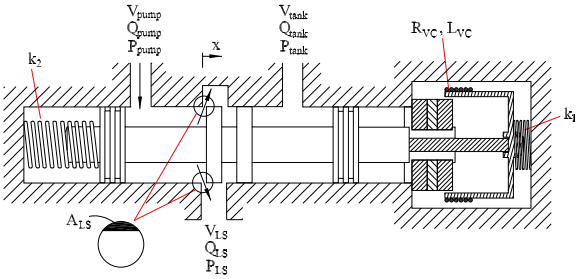

Figure 2: Model view of the spool valve with used notation.

The flows through the different valves in the system are assumed describable by the orifice equation, where, for the spool valve, also a laminar leakage term is included when opening to the pump side, as:

$$Q_{LS} = \begin{cases} C_d A_{LS}(x)\sqrt{\frac{2}{\rho}(P_P - P_{LS})} \\ \quad -K_{leak}(x)P_{LS} & , 0 \le x < x_l \\ C_d A_{LS}(x)\sqrt{\frac{2}{\rho}(P_P - P_{LS})} & , x \ge x_l \\ -C_d A_{LS}(x)\sqrt{\frac{2}{\rho}(P_{LS} - P_T)} & , x < 0 \end{cases} \quad (1)$$

Where x_l is the length of a leakage path in the spool, and $K_{leak}(x)$ is a laminar leakage coefficient. The spool dynamics is determined from the free-body diagram shown in Fig. 3.

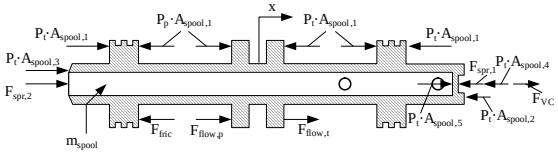

Figure 3: Forces acting on the spool.

The force equilibrium for the spool may therefore be written as follows, when noting that the spool is pressure balanced as $A_2 = A_3$:

$$m_s \cdot \ddot{x} = F_{VC} + F_{spr} - F_{f,p} + F_{f,t} - F_{fric} \quad (2)$$

Where m_s is the movable mass. $F_{f,p}$and $F_{f,t}$ are the flow forces for the pump side and tank side valve openings respectively, $F_{spr} = x\,(k_1 - k_2) + F_{spr,0}$ is the spring force and F_{fric} is the friction force. F_{VC} is the voice coil force given by eq. (4), where the current is determined from the voltage equation, i.e.:

$$u_{VC} = R_{VC} i_{VC} + L_{VC} \frac{di}{dt} + K_m \dot{x} \tag{3}$$

$$F_{VC} = K_m \cdot i_{VC} \tag{4}$$

Where K_m is the voice coil force constant and the product $K_m \dot{x}$ is the back emf.

The friction force is modelled as a combination of stiction, Coulomb and viscous friction as:

$$F_{fric} = \begin{cases} F_{VC} + F_{spr} - F_{f,p} + F_{f,t} & , (*) \\ F_c \cdot sign(\dot{x}) + B \cdot \dot{x} & , |\dot{x}| > 0 \\ (*)\ \ \dot{x} = 0 \ \wedge F_{fric} < F_s & \end{cases} \tag{5}$$

Where F_c is the Coulomb friction, F_s the stiction force and B the viscous friction coefficient, which is experimentally determined. Finally the flow forces are modelled as purely stationary flow forces, i.e. for the pump side:

$$F_{f,p} = 2 \cdot C_d \cdot A_{LS}(x) \cdot (P_P - P_{LS}) \cdot cos(\theta) \tag{6}$$

And similarly for the tank side opening. The volumes (hoses) in the system are generally described using the continuity equation, which for the LS-hose volume yields:

$$\frac{V_{LS}}{\beta} \frac{dp}{dt} + \frac{dV_{LS}}{dt} = Q_{in} - Q_{out} \tag{7}$$

With Q_{in} and Q_{out} being the flows in and out of the volume and β the effective oil bulk modulus. The latter is modelled as being pressure dependent as described in e.g. [7]. For the load the system consists of the load orifices, which are simply described by the orifice equation, whereas the on-off valve is simply modelled as a switch. The load is here only used to generate a load pressure for a given pump flow. Finally the system contains the pump, for which the model is quite comprehensive, why not included here. Details about the pump model may be found in [8].

III Verification of Model

The model has been verified based on experimentally data under different operating situations. The results of two of these tests are shown below in Figs. 4- 5. The other tests performed shows similar results.

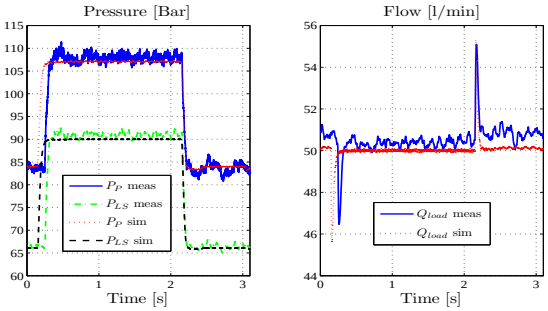

Figure 4: System response when applying load pressure steps. Notice that the first measured step is started a 0.1 [s] later than the simulation.

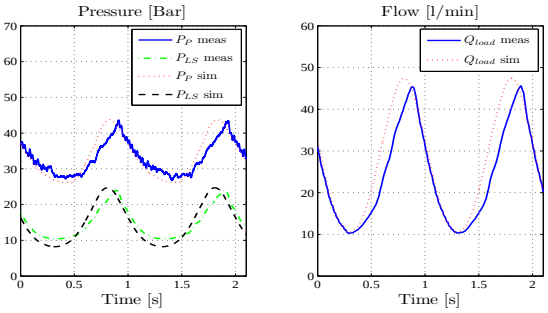

Figure 5: Sinusoidal varying 1 $[Hz]$ input.

From the results it may be seen that generally there is acceptable agreement between measured data and the simulation model, with the model showing the correct tendencies. The minor deviations result from unmodelled dynamics and the simplifications made in the the modeling process, but are within acceptable limits for the following analysis of the system and for controller design and testing.

IV Linearized Model

Based on the above non-linear model the linearized model may be derived. This is done under the approximation that the bulk modulus is constant and so are the discharge angle and discharge coefficient. Linearizing and Laplace transforming yield the following system equations:

$$m_s s^2 x = K_f i_{VC} - K_{spr,fq} x + K_{fqp,pt} P_{LS} + K_{fqp,p} P_p - Bsx \tag{8}$$

$$q_{LS} = K_x x - K_{LS} p_{LS} + k_{qp,p} p_p \tag{9}$$

$$p_{LS} = \frac{\beta}{s V_{LS}} q_{LS} \tag{10}$$

$$u_{VC} = (L_{VC} s + R_{VC})\, i_{VC} + K_{g,VC} sx \tag{11}$$

Where $K_{spr,fq} = K_{spr} + K_{fq}$, $K_x = K_{q,pt} + K_{leak,x,p}$ and $K_{LS} = K_{qp,pt} + K_{leak,p}$. Notice that for the last part of the subscript a p indicate that

the coefficient is taken for the pump side and a t for the tank side respectively (pt indicate that a coefficient is evaluated for both sides, dependent on linearization point). The first expression above describe the linearized spool force equilibrium, the second the flow to the LS-hose, the third the pressure build up in the LS-hose and the fourth the voice coil dynamics. Combining these equations in block diagram form, the block diagram shown in Fig.e 6 may be obtained.

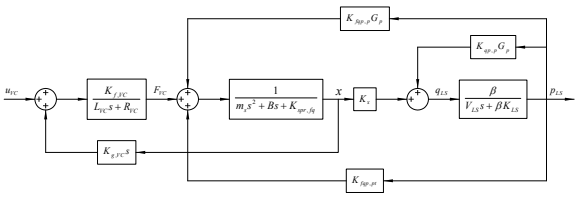

Figure 6: Block diagram relating valve voltage input ($u_{p,LS}$) to pressure in the LS-line (p_{LS}).

In the block diagram the term, $G_p(s)$, represents the pump and pump volume dynamics. As a very rough approximation this is modeled simply by a first order filter:

$$G_p(s) = \frac{p_p}{p_{LS}} = \frac{1}{\tau_p s + 1} \tag{12}$$

To simplify the following analysis, the system may be considered in two different situations, where the first is when the valve opens for connection between pump volume and the LS-hose (pump side connection), whereas the second situation is when the valve opens to tank. To further simplify the analysis the system is considered as current controlled utilizing the current control loop in the DC-DC inverter and hence neglecting the high frequency voice coil dynamics. For the case where the valve opens to the pump side the transfer function for the system may then be found to be given as:

$$\begin{aligned} G_{LS,p}(s) &= \frac{p_{LS}}{i_{VC}} \\ &= \frac{\beta K_{q,pt} K_f \left(\tau_p s + 1\right)}{G_d(s) G_m(s) - \beta \left(\left(\tau_p s + 1\right) K_{qp,t} K_{fqp,pt} + K_{q,pt}\right)} \end{aligned} \tag{13}$$

Where:

$$\begin{aligned} G_d(s) &= G_k(s)\left(\tau_p s + 1\right) - \beta K_{qp,p} \\ G_m(s) &= m_s s^2 + B s + K_{spr,fq} \\ G_k(s) &= V_{LS} s + \beta K_{qp,t} + \beta K_{leak} \end{aligned} \tag{14}$$

For the tank side connection case the system transfer function become:

$$G_{LS,t}(s) = \frac{\beta K_{q,pt} K_f}{G_k(s) G_m(s) - \beta K_{q,pt} K_{fqp,pt}} \tag{15}$$

V Stability and Sensitivity Analysis

A stability and sensitivity analysis has been conducted to determine under which operating conditions the system is most likely to become unstable, or is unstable. This is done by considering the open loop pole locations under various parameter variations, hereby investigating how the system dynamics are influenced. The operating conditions, which influence the dynamic behavior are the pressure drop over the spool valve, Δp, the spool position, x, the pump time constant, τ_p and the hose volume, V_{LS}. Similar the primary design parameters, being the spring constant, K_{spr}, spool mass, m_s, jet angle and area gradient are varied, as basis for design improvements. The main results are presented below.

A. Pump side

Considering first the pump side, the open loop pump side transfer function given in Eq. (13) has four poles and one zero. The zero originate from the pump dynamic, is always in the negative half plane and is only changed when the pump dynamics are changed, and hence of no interest at this point. Only the movement of the four poles are hence of interest. Varying the pressure drop over the spool the resulting pole place movement may be seen below.

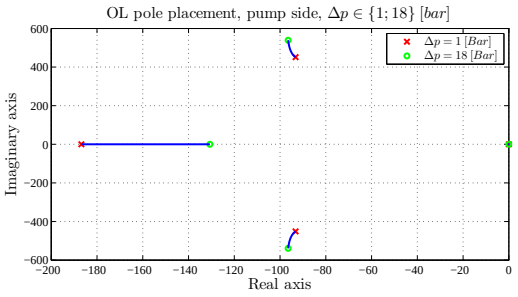

Figure 7: Varying pressure drop.

From this result it may be seen that increasing the pressure drop over the spool do not have a major influence on the dominating poles (max. pressure drop is 18 [bar]), but results in decreased damping. The worst case will hence be for the maximum pressure drop. Simulations with the nonlinear model show that the flow requirements are around 1.35 [l/min], which yields the plot shown in Fig. 8 for a varying spool position. The plot is made with basis in the limited flow requirement, as full pressure drop and large spool travel yield unrealistic high flow gains that cannot occur in the physical system.

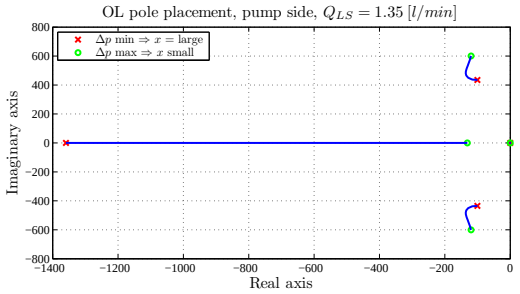

Figure 8: Pole movement for $Q_{LS} = 1.35\ [l/min]$.

Based on the above plot it is seen that an increasing spool position generally lead to lower damping and the worst case operating point for the pump side is therefore found to be for $\Delta p = 18[Bar]$ and a spool displacement $x = 0.277[mm]$.

B. Tank side

For the tank side the transfer function defined in Eq. (15) has three poles and no zeros. The pump side is here absent and hence without influence. Again the pole locations are dependent on spool position and pressure drop over spool ($\Delta p = p_{LS} - p_T$). The latter only bounded by the system pressure, why the pressure drop in opening situations may be very large. The results for the tank side are shown in Figs. 9 and 10.

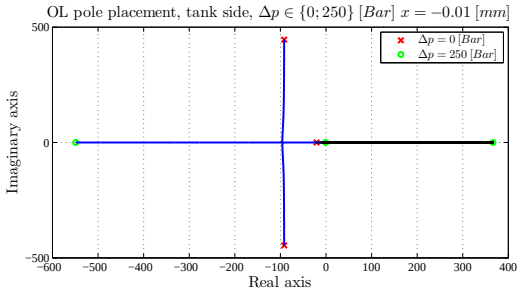

Figure 9: Pole movement varying pressure drop.

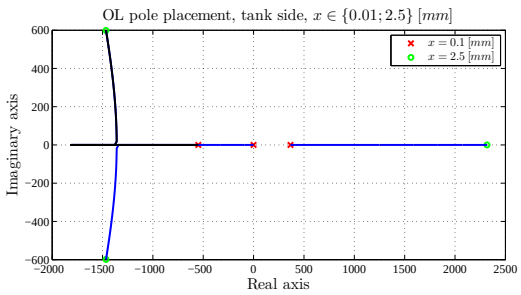

Figure 10: Varying spool position for tank side.

From the first of these plots it may be seen that for pressure drops above30 $[Bar]$ the system has one of the poles in the right half plane and is therefore defaultly unstable, which become even more outspoken for larger spool movements, cf. Fig. 10. As for the pump side, the worst case operating point is for the highest possible pressure drop and the spool displacement determined from the average flow requirement of 1.35 $[l/min]$, i.e. $\Delta p = 250[bar]$ and $x = -0.114[mm]$. The system is here unstable, and measures hence needs to be taken as discussed in the next sections, where both design and control measures are considered.

C. Sensitivity to varying System Configurations

Besides varying operating conditions, the system is also required to be robust to various system configurations , i.e. pumps and LS-hose volumes. The LS-hose volume here directly influence the open loop system gain, i.e. larger volume lower system gain, see Figs. 11-12, whereas the pump dynamics only influence the system behavior when operating on the pump side, cf. Fig. 13.

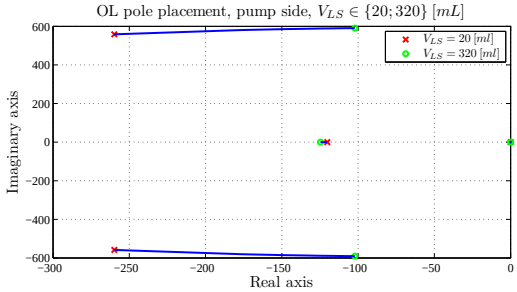

Figure 11: Pole variations for varying V_{LS}.

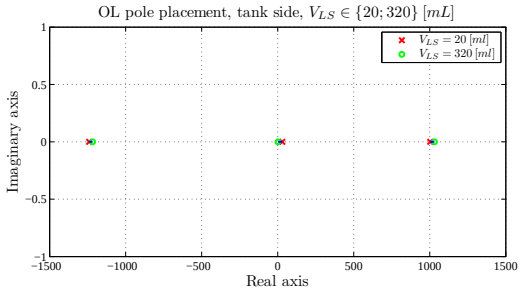

Figure 12: Tank side poles for varying V_{LS}.

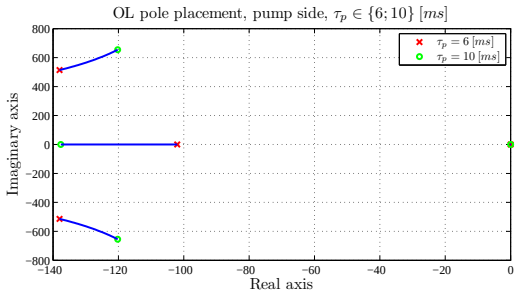

Figure 13: Pole variations for varying τ_p.

It is seen that the volume change only has minor influence on the tank side, whereas the complex poles becomes more dominating for the pump side, when increasing the volume, resulting in a less damping in the system. The same applies when the pump time constant is increased, where the damping from the complex poles reduces, but where the effect of real pole is also reduced.

D. Sensitivity to changes in Design Parameters

In the above it was found that the system is unstable when operating on the tank side. Measures hence has to be taken to stabilize the system when closing the control loop. Changing the design may, however, also have positive effects on the systems, making it possible to design less conservative controllers for stabilizing the system. The most obvious design changes are therefore considered in the following, starting with the spool mass. This is not easily lowered, but may relatively easily be increased, for which the effect is seen in Figs. 14 and 15.

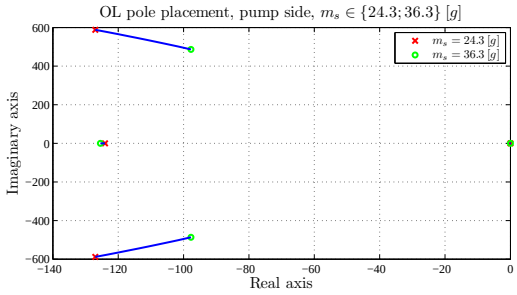

Figure 14: Pump side poles when varying spool mass.

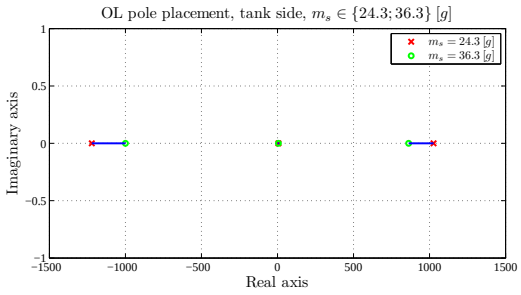

Figure 15: Tank side OL-poles for varying spool mass.

From the pump side figure it is seen that mass has significant influence on the two complex conjugate poles, hereby reducing the dominating eigenfrequency, but keeping the damping relatively unchanged. For the tank side increasing the mass slows down the system, by moving all poles closer to origo. The reduced eigenfrequency may, however, be compensated for by a higher spring constant, why in Figs. 16 and 17 the effect on the pole locations may be seen as result of varying the spring constant ± 2000 $[N/m]$ (using the original spool mass).

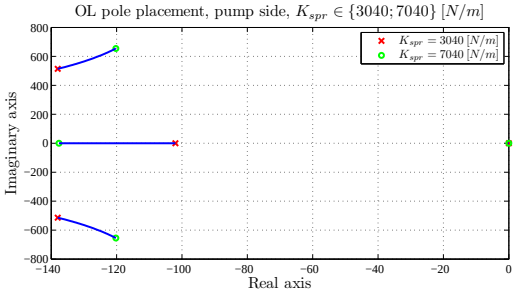

Figure 16: Open-loop poles location on pump side when considering spring constant variations.

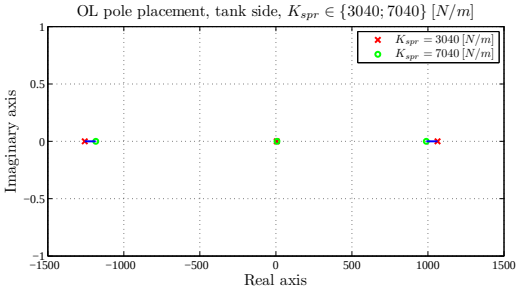

Figure 17: Open-loop poles location on tank side when considering spring constant variations.

From the graphs it may be seen that changing the spring constant has little influence on the tank side, whereas the complex poles on the pump side moves closer to the imaginary axis and away from the real axis, meaning a slightly increased eigenfrequency, but at the expense of lower system damping, which is undesirable. None of these design changes will hence benefit significantly. Changing the area gradient and/or the interrelated jet angle, shows similar results, without significant improvements, why not included, as this would also mean redesign of the spool. The last thing that could be changed is the leakage path in the valve, which may have a stabilizing effect as discussed in the following. Showing this effect is however not possible using linear analysis, as the effect is on the pump side, and the system is unstable, when operating on the tank side. As discussed in the following, this do however have the effect of limiting the pressure drop when switching over to the tank side, hereby limiting the system to operate in the stable region.

VI Controller Design and Experimental Results

The basic demands for the system is that the performance must be comparable to that of the benchmark system, whose specifications are listed below, and that the control system is robust to varying system configurations and operating conditions.

Performance specification	Value	Unit
Settling time	≤ 0.1	[s]
Maximum overshoot	0	[%]
Steady-state error	0	[bar]
Gain margin	≥ 6	[dB]
Phase margin	30-90	[°]

Table 1: System design parameters.

Basically as the system structure changes dependent on the spool position, two controllers were considered, with the switching being triggered by the spool crossing zero position. Utilizing this type of control structure, however, requires correct initialization of integrators etc. when switching structure. The problem is further complicated by the system being unstable, when operating at the tank side and with large pressure drops over the spool cf. results above. However, utilizing the leakage flow effect in the valve actively having designing the spool to have a continuous controlled leakage flow from the LS hose to tank, this problem may be reduced, as hereby the need for operating in the tank side region will be reduced to the situations with low pressure drop. Wen operating at high pressure drops, the system will instead be operating in the pump side, compensating for the high leakage flow to tank. I.e. having designed the spool to have the correct leakage flow, it will only be necessary to open to tank side, when the LS pressure is below 30 $[Bar]$, and hence the system is defaultly stable. Hereby the system dynamics may approximately be described by a relatively well damped third order system in both cases, removing the need for two controllers to obtain satisfactory performance. As the system is type zero due to the leakage flow, a standard (conservatory tuned) PI-controller is utilized to avoid steady state errors and ensuring that the controller works for both pump and tank side:

$$G_c(s) = 0.69 \cdot \left(1 + \frac{1}{1.5 \cdot s}\right) \cdot \frac{K_x}{K_{spr,fq} K_{leak,p}} \quad (16)$$

The open-loop bode plot of the system with applied PI-controller is shown in Fig. 18.

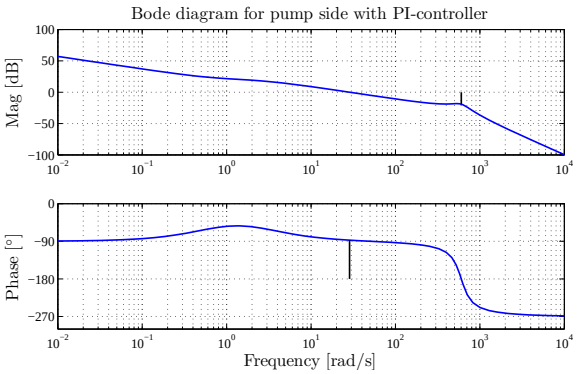

Figure 18: Bode plot of system with controller.

Based on the above analysis the designed controller has been implemented and tested experimentally under different operating conditions. The results are shown in Figs. 19-21.

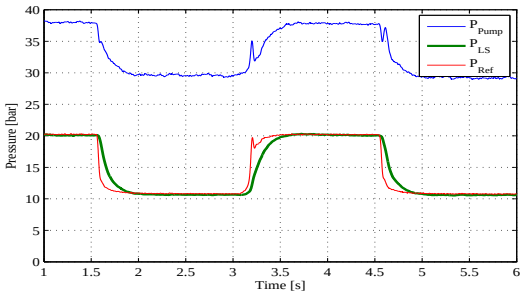

Figure 19: Measured pressure when operating at low pressures and applying pressure steps.

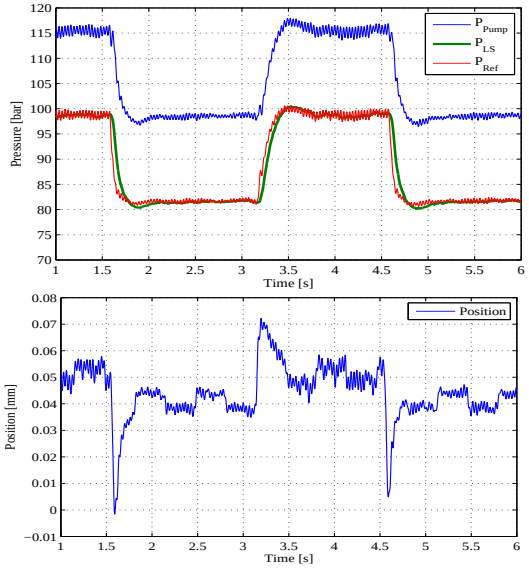

Figure 20: Measured pressure and spool position when operating at high load pressure and applying minor pressure steps.

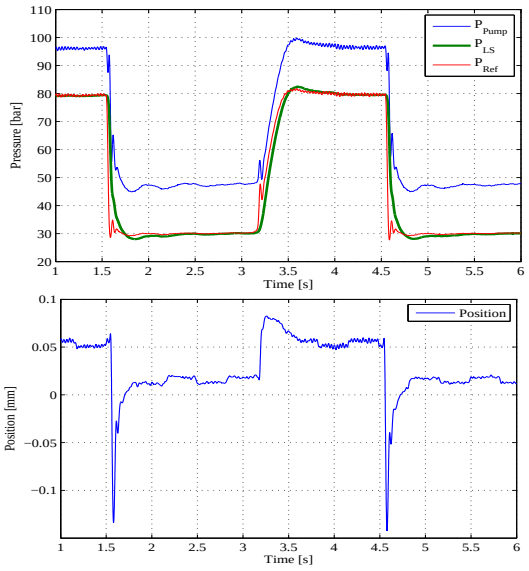

Figure 21: Measured data for high load pressure and large pressure steps.

From the results it may be seen that the system is operating as expected. For small pressure steps the system is continuously operating with a positive spool position, as seen in Fig. 20, meaning that the system is continuously controlling the leakage flow to tank. For the larger downwards pressure steps and when operating at low system pressure, see Fig. 21, the valve do switch over to the tank side to swash out the pump sufficiently fast, but in this case the pressure drop over the spool has been lowered to a level where the system is not unstable, as a result of the initial leakage flow (on the pump side).

VII Conclusion

The focus of this paper has been on generating a hydraulic (LS) pilot pressure based on an electric reference for use in systems without hydraulic feedback of the load pressure. This was done using a small spool valve, where a model of the valve and the considered system was first presented. A linear analysis of the system yielded the worst case operating conditions of the system, and based on this analysis an approach using a controlled leakage flow was utilized, hereby enabling the system to be operated with a simple PI-controller and still be stable and robust towards transitions between pump and tank side operation. Finally experimental results were presented showing the validity of the approach.

References

[1] W. Backé and B. Zähe. Electrohydraulic load-sensing. *SAE Technical Paper Series*, 1991.

[2] H. Esders. *Elektrohydraulisches Load Sensing für mobile Anwendungen.* PhD thesis, Technischen Universität Carolo Wilhelmina zu Braunschweig, 1995.

[3] H.H. Harms. Hydraulic fluid technology: Current problems and future challenges. In *International Exposition for Power Transmission and Technical Conference*, Apr. 2000.

[4] P. Krus, T. Persson, and J.-O. Palmberg. Complementary control of pressure control pumps. In *Proceedings of the IASTED International Symposium, MIC'88*, 1988.

[5] A. Langen. *Experimentelle und analytische Untersuchungen an vergesteuerten hydraulisch-mechanischen und elektrohydraulischen pumpenregulungen.* PhD thesis, Rheinisch-Westfälischen Technishen Hochshule Aachen, 1986.

[6] B. Lantto. *On Fluid Power Control - with Special Reference to Load-Sensing Systems and Sliding Mode Control.* PhD thesis, Linköping, 1994.

[7] B. Nielsen, H.C. Pedersen, T.O. Andersen, and M.R. Hansen. Modelling and simulation of mobile hydraulic crane with telescopic arm. In J.S. Stecki, editor, *1st International Conference on Computational Methods in Fluid Power Technology*, pages 145–154, Melbourne, Australia, Nov. 2003.

[8] H.C. Pedersen, T.O. Andersen, and M.R. Hansen. Designing an electro-hydraulic control module for an open-circuit variable displacement pump. In *Proc. of The Ninth Scandinavian International Conference on Fluid Power, SICFP05*, Linköping, Sweden, June 2005. SICFP05.

[9] G. Tewes and H.H. Harms. Fuzzy control for an electrohydraulic load-sensing system. In *Fluid Power Systems, Ninth Bath International Fluid Power Workshop*, Sep. 1996.

[10] B. Zähe. *Energiesparende Schaltungen hydraulischer Antrieb mit verändelichem Versorgungsdruck und ihre Regelung.* PhD thesis, Rheinisch-Westfälischen Technischen Hochschule Aachen, 1993.